

Study of Graphite Targets Interacting with
the 24 GeV Proton Beam of the BNL Muon
Target Experiment

N. Simos, H. Kirk, S. Kahn
BNL, Upton, NY 11973

K. McDonald
Princeton University, Princeton, NJ 08544

M. Cates, B. Riemer, J. Tsai, D. Beshears
ORNL, Oak Ridge, TN 37831

June 2002

STUDY OF GRAPHITE TARGETS INTERACTING WITH THE 24 GeV PROTON BEAM OF THE BNL MUON TARGET EXPERIMENT*

N. Simos[†], H. Kirk, S. Kahn, BNL, USA
K. McDonald, Princeton University, Princeton, NJ 08544, USA
M. Cates, B. Riemer, J. Tsai, D. Beshears, ORNL, USA

Abstract

A tightly focused beam on target is required in the muon collider/neutrino factory study. Specifically, up to 16 TP (1 TP = 10^{12} protons) per pulse of a 24 GeV proton beam are to be delivered on target, with a pulse length of a few microseconds and a beam spot of 1.5 mm rms sigma. Experiment E951 at BNL was set up to explore the potential of various target materials. Target integrity issues leads one to consider low-Z materials as potential targets. Thus, in the first phase of the E951 experiment, graphite and carbon-carbon composite targets were exposed to the AGS beam and their response to the induced thermal shock was studied. This paper presents theoretical prediction results as well as experimental results and makes an assessment of the abilities of prediction models to capture the dynamic response of the solid target.

1. INTRODUCTION

As part of the ongoing effort to evaluate candidate target materials for the future muon collider/neutrino factory carbon-based solid targets have been considered, both from the survivability and pion production points of view. Figure 1 depicts the meson yield for a range of incident proton energies and target materials. As part of the broad scope of experiment E951 at the AGS, solid targets were exposed to the AGS proton beam and their thermo-elastic response was studied in detail. Specifically, the muon targetry experiment calls for a 24 GeV proton beam with up to 16 TP per pulse and a pulse length of 100 ns that is tightly focused on target. The two materials selected for the experiment are ATJ graphite and the anisotropic carbon-carbon composite. Each target consists of a pair of 16mm diameter rods placed in line with the proton beam. Figures 2 and 3 depict the schematic and actual arrangements respectively. Each of the ATJ graphite rods is 30-cm long resulting in a total target length of 60 cm. The carbon-carbon rods are 12 cm long each resulting in a target length of 24 cm. A key property of the carbon-carbon composite explored in this experiment is the low coefficient of thermal expansion which, when combined with its high mechanical strength, makes it a favorable target candidate. Theoretical predictions of the response

of the ATJ graphite targets, through a transient thermal and stress wave propagation formulations, were made and are compared to the experimental results. These predictions incorporated energy deposition rates which were independently calculated by the hadron interaction codes MARS and GEANT. The thermal response and the subsequent stress wave generation and propagation were computed using transient finite element analysis procedures (ANSYS). For the actual experiment, the carbon targets exposed to the AGS proton beam were instrumented with fiberoptic strain gauges that were to record the dynamic axial strains induced by the thermal pulse.

With the help of the predicted and experimental data key issues such as, a) the verification of the low thermal expansion property of the carbon-carbon composite, b) the confirmation of the ability of the hadron interaction codes (MARS & GEANT) in predicting energy deposition on the targets based on the various combinations of proton beam intensity and spot size, and c) the confirmation of the ability of the adopted analytical model in predicting the target response are addressed.

2. E951 EXPERIMENT

2.1 Strain Measurement Set-Up

The goal of the experiment involving the carbon targets was to measure the strains at the surface of the targets and compare them with analytical predictions. A good agreement of the behavior and amplitude of strain will indicate that the simulation model is appropriate and thus able to predict the state of stress and survivability of the target. To measure the strain the ATJ and carbon-carbon composite targets shown in Figures 2 & 3 have been instrumented with fiberoptic strain gauges. Specifically, the ATJ graphite rods was instrumented with eight (8) gauges (four at mid-length at 90 deg. apart, and two near the front and back 180 deg. apart respectively). The arrangement of the gauges in the middle of each ATJ target is to help identify the actual beam line relative to the target centerline. Three strain

* Work performed under the auspices of the US DOE

[†] simos@bnl.gov

gauges were placed in the front carbon-carbon rod and two in the rear. All gauges were set to record axial strains. These strain gauges are designed around an interferometer by FISO Technologies Inc.

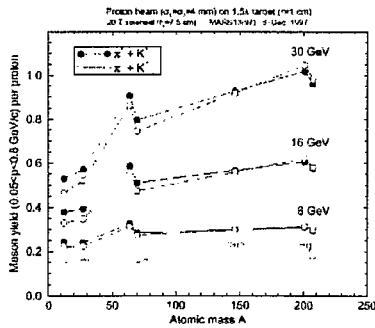


Figure 1. Meson yield for various target materials

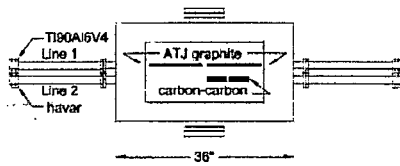


Figure 2: Schematic plan-view of target arrangement

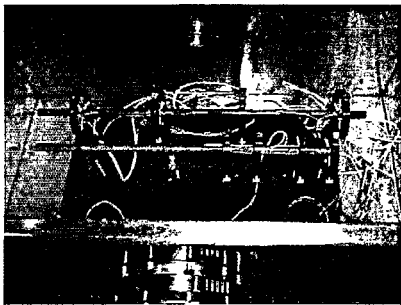


Figure 3: Instrumented targets in the E951 enclosure

The basic active element (cavity) consists of two mirrors facing each other. The direct output is a 100 KHz signal. However, when the acquired signal goes through a custom-made filtering that is based on signal de-composition and re-construction, a 500 KHz strain signal is deduced. The wavelength of the induced shock front and the ability of acquisition system to capture it is vital for strain amplitude and time structure assessment.

2.2 Strain Measurements

In the course of the carbon target tests of the E951 experiment beam intensities up to 3.1 TP was delivered on target. Based on activation analysis of the beam windows of the target space (see Fig. 2) the corresponding beam spot size was of the order of 0.3mm x 1mm rms.

Figures 4 through 7 depict actual strains recorded by the strain gauges. Specifically, Figures 4 & 5 are associated with 1.7 TP proton beam and the tighter of the two spots and they show strains in the middle of the front ATJ rod at gauges 1 & 3 which are 180 deg apart. As expected, the two are out of phase as soon as the bending modes are excited. As shown in Figure 5, for a few axial vibration cycles the two locations move together. Figure 6 depicts strains also in the middle of the front target rod and at locations 180 deg apart. The responses are in phase implying that the target bends about the axis connecting them. Figure 7 compares strains in the middle of the two ATJ rods. It can be clearly seen that the proton beam has been significantly dispersed by the time it reaches the back target rod.

Dispersion of the generated stress pulse can be seen in the recorded strains. This is due to both material damping and friction loss at the interface of the target with its collar-like supports.

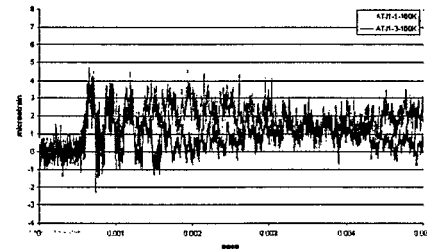


Figure 4: Strains in the front ATJ rod (180° apart)

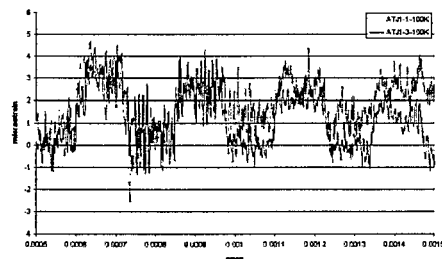


Figure 5: Initial strain cycles of record in Fig. 5

Analytical calculations confirmed the fundamental periods for radial, axial and bending modes. Specifically, the observed bending frequency in the ATJ targets is approximately 390 Hz and the calculated is 395Hz. The axial “ringing” period observed is approximately 265μs and the calculated period is of the order of 261μs.

Figure 8 depicts the finite element analysis results in the middle of the front rod based on 1.7 TP beam and the revised spot (0.3mm x 1mm rms). While uncertainties regarding the offset of the proton beam and the spot size still exist, the prediction results compare well with the experimental results of Fig. 5. One should note that no dispersion other than geometric was introduced in the finite element analysis. Figures 8 and 9 depict prediction and actual results near the front end of the

first ATJ rod. While there is excellent agreement in the “structure” of the response, there is discrepancy in the amplitude. This discrepancy is attributed to the offset of the beam.

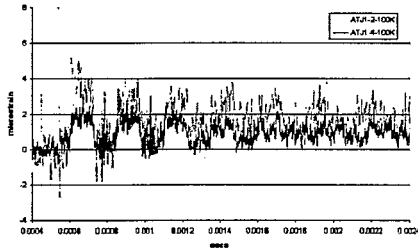


Figure 6: Strains in the middle of the front rod

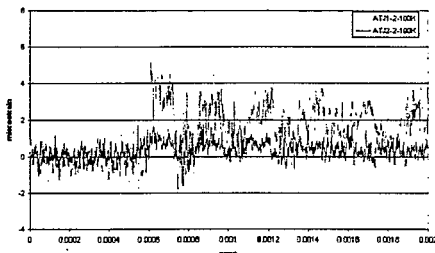


Figure 7: Strain comparison in the two ATJ rods

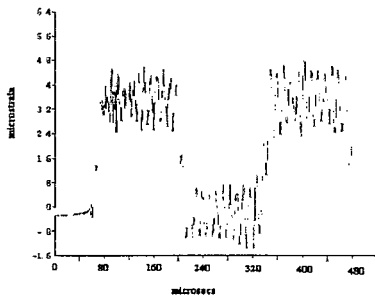


Figure 8: Predicted strains in the front ATJ rod

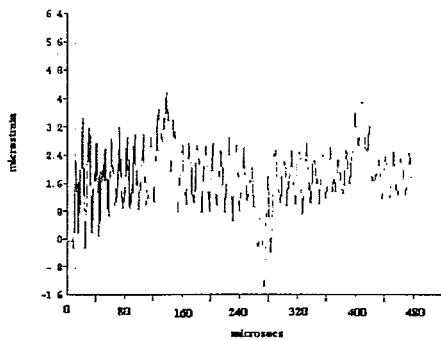


Figure 9: Predicted strains near the front-end

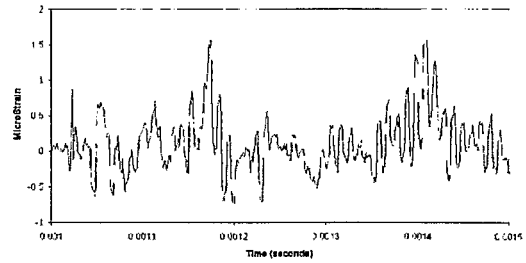


Figure 10: Measured strains near the front-end

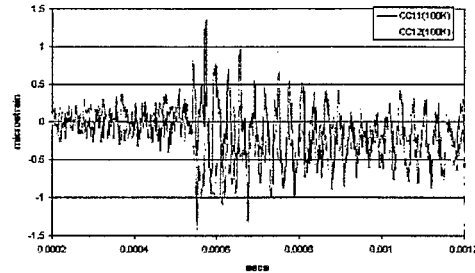


Figure 11: Measured strains in the carbon composite

Of great importance are the strains observed in the carbon-carbon composite. As seen in Fig. 11, the strains observed are about five times less than those seen in the ATJ graphite. It is further observed that the composite still responds dynamically to a fast beam. Its useful property of almost no thermal expansion apparently applies to slow heating processes.

3. SUMMARY

The experimental effort on solid carbon targets generated strain measurements that are being used to confirm the validity of the prediction model that is based on finite element procedures. Aside of the uncertainties of the beam focusing and line of action relative to the centerline of the targets, the measurements are in very good agreement with the strain levels predicted by the model. This implies that the model can be used to predict the response and survivability of the solid targets under far more severe conditions that are called by the muon collider study.

REFERENCES

- [1] D. Burgreen, “Thermoelastic Dynamics of Rods, Thin Shells and Solid Spheres”, Nucl. Sc. And Eng., 12, 203-217, 1962
- [2] N.V. Mokhov, “The MARS Code System User Guide, Version 13 (95)”, 1995
- [3] K. F. Graff, “Wave Motion in Elastic Solids,” Ohio State University Press, 1975
- [4] ANSYS Engineering Analysis of Systems, Swanson Analysis Systems Inc., 1999